Macromolecular Materials and Engineering
www.mme-journal.de

High Stiffness Cellulose Fibers from Low Molecular Weight Microcrystalline Cellulose Solutions Using DMSO as Co-Solvent with Ionic Liquid

Chenchen Zhu, Anastasia F. Koutsomitopoulou, Stephen J. Eichhorn, Jeroen S. van Duijneveldt, Robert M. Richardson, Rinat Nigmatullin, and Kevin D. Potter*

There is a need to develop high-performance cellulose fibers as sustainable replacements for glass fibers, and as alternative precursors for carbon filaments. Traditional fiber spinning uses toxic solvents, but in this study, by using dimethyl sulfoxide (DMSO) as a co-solvent with an ionic liquid, a novel high-performance fiber with exceptional mechanical properties is produced. This involves a one-step dissolution, and cost-effective route to convert high concentrations of low molecular weight microcrystalline cellulose into high stiffness cellulose fibers. As the cellulose concentration increases from 20.8 to 23.6 wt%, strong optically anisotropic patterns appear for cellulose solutions, and the clearing temperature (T_c) increases from ≈100 °C to above 105 °C. Highly aligned, stiff cellulose fibers are dry-jet wet spun from 20.8 and 23.6 wt% cellulose/1-ethyl-3-methylimidazolium diethyl phosphate/DMSO solutions, with a Young's modulus of up to ≈41 GPa. The significant alignment of cellulose chains along the fiber axis is confirmed by scanning electron microscopy, wide-angle X-ray diffraction, and powder X-ray diffraction. This process presents a new route to convert high concentrations of low molecular weight cellulose into high stiffness fibers, while significantly reducing the processing time and cost.

1. Introduction

As the most abundant natural polymer worldwide,[1–4] cellulose has numerous advantages, including low cost, sustainability, renewability, biocompatibility, and biodegradability.[5] It is however not used in large-scale industrial composite applications because it cannot be melt-processed and is insoluble in nearly all aqueous and organic solvents.[6] This insolubility is due to its complex intra- and intermolecular hydrogen bonding network[7,8] and, possibly, hydrophobic interactions.[9,10] The use of traditional aromatic and halogenated solvents for cellulose has been reduced noticeably in organic synthesis and industrial chemical processes due to their safety requirements.[11] Ionic liquids (ILs) are considered as a new class of solvents for cellulose due to their chemical and thermal stabilities,[12,13] reusability,[14] and dissolution performance.[15–19] A specific IL, 1-ethyl-3-methylimidazolium diethyl phosphate (EMImDEP), has been selected as a solvent in this study due to its numerous advantages, including low melting point,[20,21] high hydrogen bond acceptor capability,[22] as well as its comparatively low viscosity (284 cP at 40 °C).[23] These properties of EMImDEP can enhance the fiber spinning process in order to produce high-performance cellulose fibers,[24] despite some moderate hazards including acute toxicity (e.g., oral, dermal, and inhalation), skin irritation and sensitization, as well as specific targeted organ toxicity under a single exposure.Dimethyl sulfoxide (DMSO) is a low-cost, nontoxic polar aprotic solvent, which is miscible in a wide range of solvents including ILs.[6,25,26] Working as a co-solvent with an IL, it can reduce the dissolution time, and temperature (T),[27] as well as the viscosity of cellulose solutions without precipitation,[25] thus improving dissolution.[6,26] The addition of DMSO can improve the breakdown of the ionic association of $EMIm^+DEP^-$ by solvation of the cation $EMIm^+$ and anion DEP^-.[28] The more the ions are dissociated, the more active $EMIm^+$ and DEP-ions are available to deconstruct the hydrogen bonding network of cellulose, while also forming new hydrogen bonds with cellulose[6,7,26,29–34] thus improving its dissolution.[35] Moreover, with the addition of low-cost DMSO, the expense of the cellulose

Dr. C. Zhu, Dr. A. F. Koutsomitopoulou, Prof. S. J. Eichhorn, Dr. R. Nigmatullin, Prof. K. D. Potter
Bristol Composites Institute (ACCIS)
Department of Aerospace Engineering
University of Bristol
Queen's Building University Walk
Bristol BS8 1TR, UK
E-mail: Chenchen.Zhu@bristol.ac.uk
Dr. J. S. van Duijneveldt
School of Chemistry
University of Bristol
Cantock's Close, Bristol BS8 1TS, UK
Prof. R. M. Richardson
HH Wills Physics Laboratory
Physics Department
University of Bristol
Tyndall Avenue, Bristol BS8 1TL, UK
The ORCID identification number(s) for the author(s) of this article can be found under https://doi.org/10.1002/mame.201800029.

DOI: 10.1002/mame.201800029

solvent can be significantly decreased due to a reduced quantity of EMImDEP (currently ≈50 times more expensive per liter) required for dissolution.

2. Results and Discussion

In this study, stiff cellulose fibers were manufactured from optically anisotropic solutions by dissolving low molecular weight microcrystalline cellulose (degree of polymerization = 200–220;[36,37] molecular weight equivalent ≈75 240 g mol^{-1}), which is usually used for low mechanical property applications (medical tablets, foodstuffs, etc.). Critically, we use DMSO as a co-solvent with EMImDEP to achieve this, generating a new approach to dissolution and the formation of high-performance fibers.

To compare the cellulose dissolving capability, Kamlet–Taft parameters of EMImDEP/DMSO mixtures with different ratios were investigated at 10–70 °C (**Figure 1**; Figure S1, Supporting Information). The two essential characteristics required to improve the dissolution of cellulose are the increased hydrogen bond accepting ability (β) and decreased hydrogen bond donating ability (α). As a reasonable empirical descriptor, net basicity ($\beta - \alpha$ as a function of β)[38–40] at 70 °C (the closest T to our dissolution T) was investigated with fitting accuracy as shown in Figure 1, indicating a best mass fraction of EMImDEP/DMSO = 7:3 (Figure 1). The concentrations of microcrystalline cellulose (20.8 and 23.6 wt%) were optimized to achieve optically anisotropic solutions contributing to the alignment of cellulose chains. Similarly, multiple fiber extrusion/winding draw ratios (DR = 3.5, 4.0, 4.5, and 5.0) were used to further improve this alignment during the dry-jet wet spinning of our stiff cellulose fibers. This study presents a controllable and cost-effective route to produce high-performance engineering cellulose fibers using an IL/co-solvent system.

The 20.8 and 23.6 wt% cellulose solutions were observed using a polarized optical microscope at various temperatures

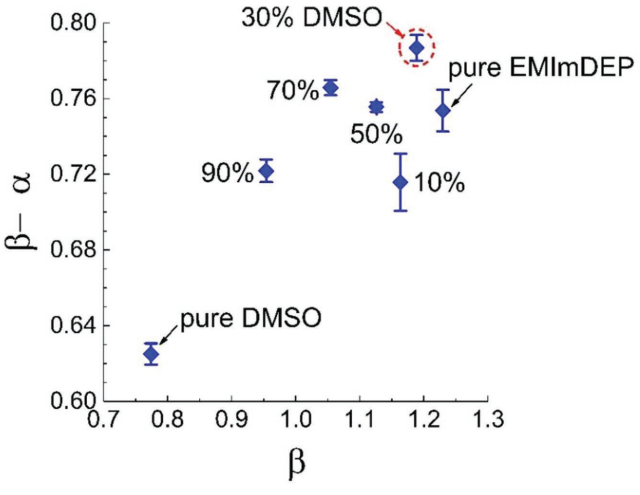

Figure 1. Net-basicity $\beta - \alpha$ plotted against β for EMImDEP/DMSO solvent mixtures with various DMSO ratios (0, 10%, 30%, 50%, 70%, 90%, and 100%) at 70 °C. Error bars are determined from fits to the underlying data.

(T = 25–105 °C) to investigate their anisotropic behavior (Figure S2, Supporting Information). For both solutions, strong optical planar textures were observed, which are typical signatures of anisotropy. These were observed at 25 °C and diminished gradually as T increased. The diminishing textures indicate the nematic cellulose solutions approach to an isotropic transition, which is attributed to the reduced resistance (generated by shear viscosity) on the orientation of cellulose chains to the migration into a random state.[7,24,41] The anisotropy pattern finally disappeared at a clearing temperature (T_c)[42] of 100 °C for the 20.8 wt% solution (Figure S2, Supporting Information). However, it remained strong at 105 °C for the 23.6 wt% solution (**Figure 2**a), which is higher than has been previously reported,[24,42,43] indicating better self-accessibility of cellulose chains dispersed in EMImDEP. The difference in T_c for cellulose solutions also suggests that during the fiber spinning process at 100 °C in this study, the 20.8 wt% fibers were produced from isotropic solutions, while the 23.6 wt% fibers were produced from an anisotropic solution. That could explain the significantly higher mechanical properties of fibers produced at 23.6 wt% cellulose compared to those produced at 20.8 wt%.

When the cellulose/EMImDEP/DMSO solution is extruded through the nozzle during fiber spinning, a predominantly shear-free uniaxial extensional flow and a shear flow occur simultaneously within the spin-line of the solution dope before entering the coagulation bath. A rheological study in shear is the simplest method to reveal the properties of the fiber spinning solution,[47] as well as helping to improve the flow rate control in a fiber manufacturing process.[48] The steady shear viscosity (η) curves as a function of the shear rate (γ) are shown in Figure 2b for 20.8 and 23.6 wt% cellulose/EMImDEP/DMSO solutions. The shapes of both curves are typical for polymer solutions, with a Newtonian region at low shear rates and a reducing viscosity with an increasing shear rate. The values of zero-shear viscosity were found to be 39.2 and 72.8 Pa s for the 20.8 and 23.6 wt% solutions, respectively.

Scanning electron microscope (SEM) images were taken to examin the cross sections (perpendicular to the fiber axis) and the outer surfaces of the cellulose fibers (Figure 2e and **Figure 3**; Figure S5, Supporting Information). Smooth outer surfaces were observed for 20.8 wt% fibers (Figure 3a(1),(2)), while striations along the fiber lengths were observed for 23.6 wt% fibers, especially at high DR (Figure 3a(3),(4); Figure S5, Supporting Information). These striations could be an indication that orientation of the filaments occurred, producing a fibrillar morphology; this can be modulated by varying the cellulose concentration and DR.[49] The striations on the surface of the 23.6 wt% fiber could potentially contribute to their physical bonding with resins in composite materials. All cross sections appear to be circular (Figure 3b) without any visible large-sized voids (Figure 3c). Surrounded by a thin skin of material (Figure 3c), the core structures throughout the cross sections appear uniform and independent of the blend ratio of cellulose and EMImDEP/DMSO (Figure 3b), indicating their compatibility. This compatibility could crucially contribute to the full stretching of macromolecular cellulose chains in the fibers; increasing the number of hydrogen bonds between cellulose and water during coagulation, while restraining the diffusion velocity of water to generate uniform fiber structures.[50–52] The

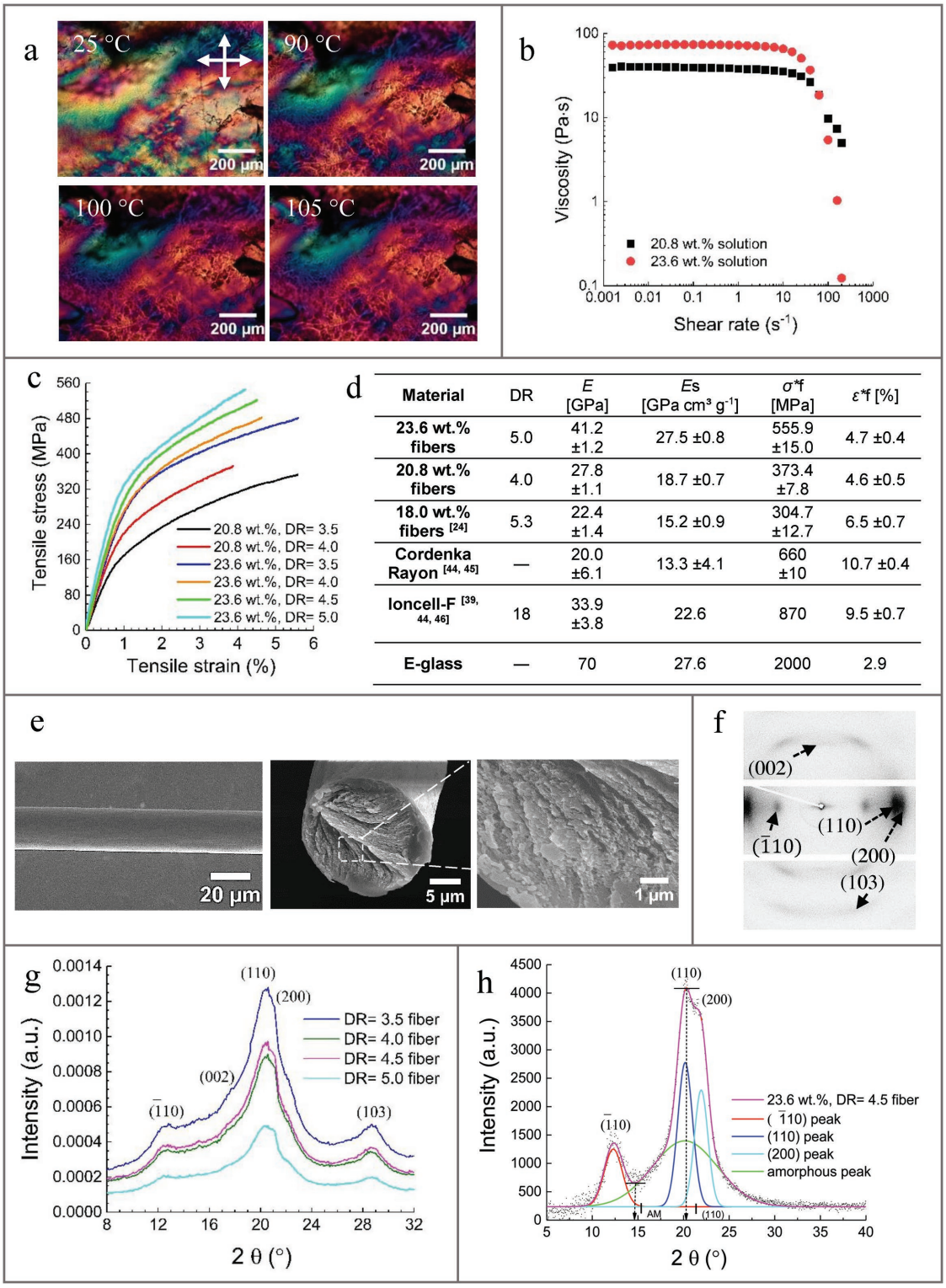

Material	DR	*E* [GPa]	*Es* [GPa cm³ g⁻¹]	σ*f [MPa]	ε*f [%]
23.6 wt.% fibers	5.0	41.2 ±1.2	27.5 ±0.8	555.9 ±15.0	4.7 ±0.4
20.8 wt.% fibers	4.0	27.8 ±1.1	18.7 ±0.7	373.4 ±7.8	4.6 ±0.5
18.0 wt.% fibers [24]	5.3	22.4 ±1.4	15.2 ±0.9	304.7 ±12.7	6.5 ±0.7
Cordenka Rayon [44, 45]	—	20.0 ±6.1	13.3 ±4.1	660 ±10	10.7 ±0.4
Ioncell-F [39, 44, 46]	18	33.9 ±3.8	22.6	870	9.5 ±0.7
E-glass	—	70	27.6	2000	2.9

Figure 2. a) Typical polarized optical microscopic images of 23.6 wt% cellulose/EMImDEP/DMSO solutions at $T = 25$–105 °C. b) Viscosity flow curves for 20.8 and 23.6 wt% cellulose/EMImDEP/DMSO solutions at 100 °C. c) Typical tensile stress–strain curves of 20.8 and 23.6 wt% cellulose fibers produced using different draw ratios (DR) (3.5, 4.0, 4.5, and 5.0). d) Young's modulus (E), specific Young's modulus (E_s), breaking stress (σ^*_f), and breaking strain (ε^*_f) of 20.8 wt% (DR = 4.0) and 23.6 wt% cellulose fibers (DR = 5.0) compared to our previously produced 18.0 wt% cellulose fibers (DR = 5.3), commercial cellulose fibers and E-glass. e) Morphology of outer surfaces, cross sections, and cross sections under higher SEM magnification of 23.6 wt% cellulose fibers (DR = 5.0). f) Wide-angle X-ray diffraction (WAXD) patterns of 23.6 wt% cellulose fibers (DR = 5.0). g) WAXD radial data for 23.6 wt% cellulose fibers (DR = 3.5, 4.0, 4.5, and 5.0). h) Powder X-ray diffraction (XRD) spectra highlighting crystalline diffraction peaks ($\bar{1}10$), (110), and (200) and the amorphous phase of 23.6 wt% cellulose fibers (DR = 4.5).

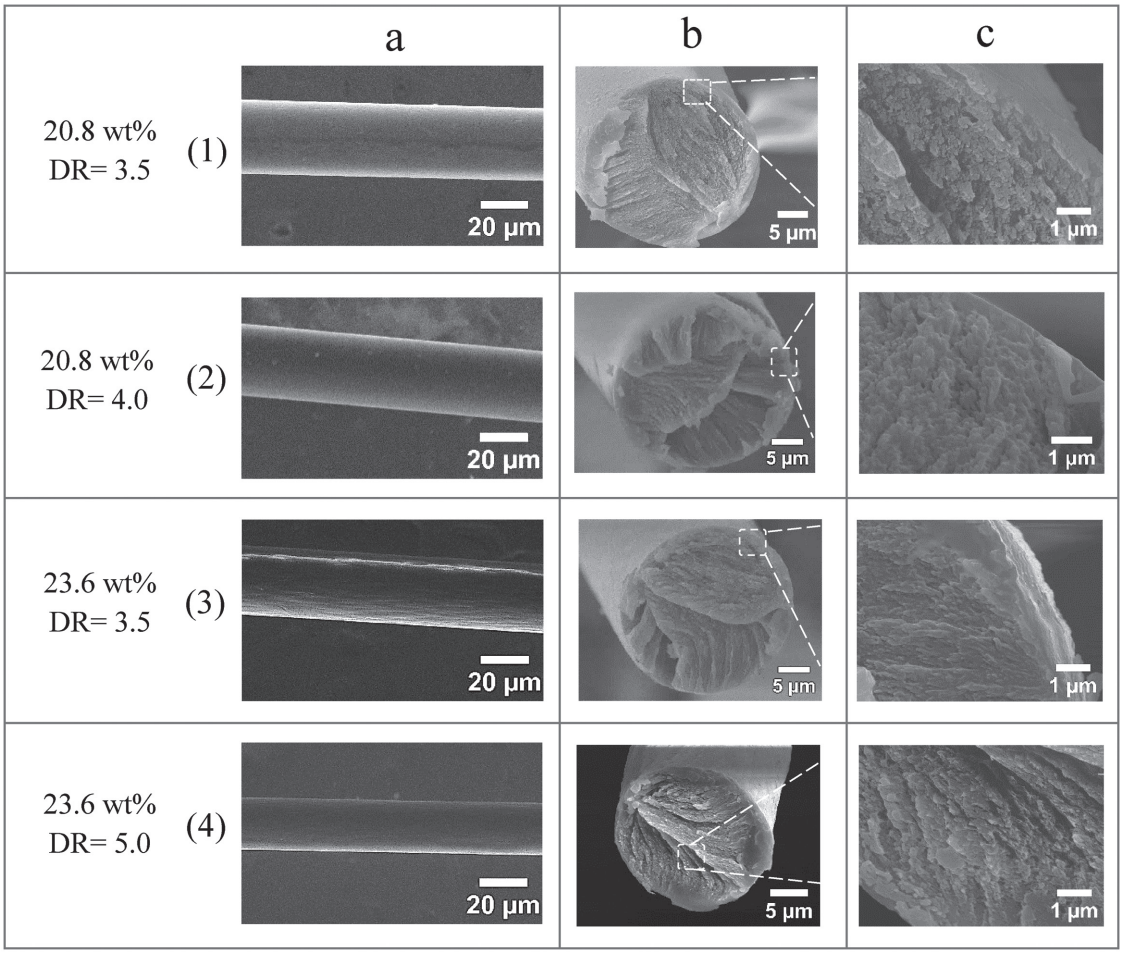

Figure 3. Typical scanning electron microscopic (SEM) images of the fibers showing the morphology of the a) outer surfaces, b) cross sections, and c) cross sections under higher magnifications for 20.8 wt% (DR = 3.5 and 4.0) and 23.6 wt% (DR = 3.5 and 5.0) cellulose fibers.

cylindrical cores of fibers (Figure 3b) in this study look much denser than our previous fibers,[24] which may be due to the increased cellulose concentration.

To study the cellulose structure and chain alignment in the fibers, single filaments of both 20.8 and 23.6 wt% samples were analyzed using wide-angle X-ray diffraction (WAXD) with a wavelength of 0.154 nm (Cu Kα radiation; Figure S6, Supporting Information). The Bragg peaks observed from 2D WAXD diffraction patterns (Figure 2f) are typical of a cellulose II structure, a widely accepted crystal structure of regenerated cellulose.[53,54] The most intense peak (110) for our cellulose fibers shifted to a 2θ angle of 20.6° from around 22.5°, which is the typical position of this Bragg peak for cellulose I. This is indicative of a nonrecoverable change in the cellulose lattice structure after regeneration due to the diffused IL.[55] The ($\bar{1}$10) peak at 12.8° is also indicative of a transformation to a cellulose II structure after regeneration (Figure 2g).

The cellulose II monoclinic $P2_1$ structure unit cell dimensions of our fibers were calculated using measured Q values of the ($\bar{1}$10), (110), (002), (200), and (103) cellulose planes from the WAXD patterns (Table S1, Supporting Information).[24] Our determined unit cell dimensions are in good agreement with average literature values for cellulose II (a = 0.911 nm, b = 0.796 nm, c = 1.034 nm, $\alpha = \beta$ = 90° and γ = 117.4°).[56] The slight differences may be due to numbers of diffraction peak intensities overlapping each other in the X-ray data.[57]

In the fibers, the cellulose chains have a preferred orientation along their longitudinal axes parallel to the deformation direction. The preferred orientation appears as a concentrated intensity of two arced diffraction rings, in the azimuthal direction (Figure 2f; Figure S6, Supporting Information). The intensity distribution of a ring containing the ($\bar{1}$10) peak, with the background estimated from adjacent rings and subtracted using IDL, were plotted as a function of azimuthal angle and fitted using a Lorentzian function (Figure S6, Supporting Information). For comparison with literature values, multiple values quantifying the extent of crystalline orientation in our fibers, including Herman's orientation factor (f), were calculated from these intensity distributions[24] (Table S1, Supporting Information). The details on how these values are calculated are discussed in our previous study.[24] A higher degree of alignment of the cellulose chains possesses a higher f value (Table S1, Supporting Information). All orientation values indicate that the 23.6 wt% fibers (DR = 5.0) possess the highest orientation of cellulose chains along the fiber axis (f = 0.84). This value of f is much higher compared to our previously published study

(18.0 wt% fibers (f = 0.80)) and similar to Ioncell-F fibers (DR = 14.1) (f = 0.82).[39]

To estimate the crystallinity, for 20.8 wt% (DR = 3.5) and 23.6 wt% (DR = 4.5) fibers, powder X-ray diffraction (XRD) analyses were conducted while samples were rotated on a spinning stage to overcome preferred orientation (Figure 2h; Figure S7, Supporting Information). After background subtraction, the crystallinity indices (*CrI*) were calculated using a peak height method developed by Segal (Equation (S6), Supporting Information) for the comparison of similar structure materials prepared in our previous study.[24,58] We also used a peak fitting method[59,60] (Equation (S7), Supporting Information) for comparison with literature values, since Segal's method has recently been shown to yield erroneous results.[61] Using Segal's method, the *CrI* values are 85.5% for 20.8 wt% (DR = 3.5) fibers and 83.9% for 23.6 wt% (DR = 4.5) fibers (Table S1, Supporting Information); both values are much higher than the 64.4–66.8% range from our previous cellulose fibers (12.4–18.0 wt%).[24] However, the high *CrI* values may be due to the underestimation of the amorphous fraction for cellulose II.[62] The powder XRD data for our cellulose fibers and their diffraction peaks were fitted using a Gaussian function; these fits gave correlation coefficients (R^2) of 0.96 for 20.8 wt% (DR = 3.5) fibers and 0.99 for 23.6 wt% fibers. Using the peak fitting method, the *CrI* values were found to be 54.1% and 52.5% for 20.8 wt% (DR = 3.5) and 23.6 wt% (DR = 4.5) fibers (Table S1, Supporting Information).

To study the physicomechanical properties of 20.8 and 23.6 wt% cellulose fibers, their average diameters (d) were measured, and mechanical properties were tested (Figure 2c,d; Figure S4a and Table S1, Supporting Information). The 23.6 wt% (DR = 5.0) cellulose fibers possess the smallest average diameter of 18.2 ± 1.3 µm, lower than the diameters (20.8 ± 3.0 µm) obtained from our previous 18.0 wt% fibers[24] (Table S1, Supporting Information). For 20.8 and 23.6 wt% fibers, as the DR was increased from 3.5 to 4.0, respectively, Young's modulus (E) increased sharply to 27.8 ± 1.1 GPa (8.2% increment) and 35.5 ± 2.2 GPa (10.6% increment). Breaking stress (σ^*_f) appeared little changed at 373.4 ± 7.8 MPa (2.1% increment) and 483.2 ± 26.5 MPa (0.3% reduction). Breaking strain (ε^*_f) decreased as expected to 4.6 ± 0.5% (11.5% reduction) and 5.0 ± 0.3% (15.3% reduction) (Figure 2c; Figure S4b–d and Table S1, Supporting Information). As the DR was further increased to 5.0 for the 23.6 wt% fibers, Young's modulus also increased to 41.2 ± 1.2 GPa and σ^*_f increased to 555.9 ± 15.0 MPa, both of which are more than 82% higher than our previous 18.0 wt% cellulose fibers[24] (Figure 2c,d). This increase in mechanical properties is thought to be due to a higher concentration of cellulose being successfully dissolved with the addition of DMSO, resulting in an overall major contribution to the properties of the regenerated cellulose fibers developed in this study. The highest achieved Young's modulus (E) of our fibers is twice that of Cordenka fibers and 21.5% higher than Ioncell-F fibers (DR = 15 and 18) (Figure 2c). Moreover, considering that the density of the cellulose fibers produced in this study is probably ≈1.4–1.5 g cm^{-3}, the specific Young's modulus (E_s = E/density) of our best fibers is probably ≈28 GPa cm^3 g^{-1}, which is about the same as E-glass fibers (27.6 GPa cm^3 g^{-1}) (Figure 2d). Regenerated cellulose fibers with exceptional mechanical properties, called Bocell, have been, previously, independently reported by Northolt et al. (E = 44 GPa, σ^*_f = 1.7 GPa)[63] and Eichhorn et al. (E = 42 GPa, σ^*_f = 1.1 GPa).[64] However, the dissolution process to produce Bocell fibers was relatively complex compared to our approach, involving orthophosphoric acid, pyrophosphoric acid, polyphosphoric acid, phosphorus pentoxide, and water.

3. Conclusions

In summary, a novel and cost-effective route was presented to manufacture high stiffness cellulose fibers from anisotropic solutions by dissolving high concentrations of low molecular weight microcrystalline cellulose using DMSO as a co-solvent with IL EMImDEP. The processing time (solution preparation and degassing) to produce the cellulose fibers has been significantly reduced from 42 h in our previous study[24] to only 6 h, which significantly boosts the manufacturing efficiency. Both 20.8 and 23.6 wt% cellulose/EMImDEP/DMSO solutions showed a strong sign of anisotropy with T_c increasing above 100 °C. The values of their zero-shear viscosity are 39.2 and 72.8 Pa s, respectively. WAXD and tensile testing of 20.8 and 23.6 wt% cellulose fibers at various DR confirmed that 23.6 wt% cellulose fiber (DR = 5.0) possessed the highest crystal orientation and therefore mechanical properties (E = 41.2 GPa; σ^*_f = 555.9 MPa). Despite using a low molecular weight cellulose, superior specific modulus (27.5 GPa cm^3 g^{-1}) was achieved similar to E-glass fibers (27.6 GPa cm^3 g^{-1}). These findings create a potential route to convert low-performance cellulose waste into high-performance fibers for composite materials as well as precursors for carbon fibers. The anisotropic behaviors of our cellulose/EMImDEP/DMSO solutions during the spinning procedure will be investigated in future work as the final proof of the spinning of a liquid crystalline cellulose solution.

4. Experimental Section

For all the experimental details, please see the Supporting Information.

Supporting Information

Supporting Information is available from the Wiley Online Library or from the author.

Acknowledgements

The authors would like to acknowledge funding from the Engineering and Physical Science Research Council (EPSRC, grant code EP/L017679/1). The authors thank Dr. Jean-Charles Eloi and Dr. Sean Davis for help with SEM studies carried out in the Chemical Imaging, University of Bristol, with equipment funded by EPSRC under Grant "Atoms to Applications" (EP/K035746/1). The Ganesha X-ray scattering apparatus located in the School of Physics, University of Bristol, was also supported through the EPSRC Grant "Atoms to Applications." All data can be downloaded for free from the University of Bristol's repository at https://data.bris.ac.uk/data/.

Conflict of Interest

The authors declare no conflict of interest.

Keywords

anisotropy, dimethyl sulfoxide, fiber spinning, ionic liquid, microcrystalline cellulose

Received: January 12, 2018
Revised: February 14, 2018
Published online:

[1] D. N. Saheb, J. P. Jog, *Adv. Polym. Technol.* **1999**, *18*, 351.
[2] H. Yang, R. Yan, H. Chen, D. H. Lee, C. Zheng, *Fuel* **2007**, *86*, 1781.
[3] A. Pinkert, K. N. Marsh, S. Pang, M. P. Staiger, *Chem. Rev.* **2009**, *109*, 6712.
[4] T. Arioli, L. Peng, A. S. Betzner, J. Burn, W. Wittke, W. Herth, C. Camilleri, H. Höfte, J. Plazinski, R. Birch, A. Cork, J. Glover, J. Redmond, R. E. Williamson, *Science* **1998**, *279*, 717.
[5] R. J. Moon, A. Martini, J. Nairn, J. Simonsen, J. Youngblood, *Chem. Soc. Rev.* **2011**, *40*, 3941.
[6] D. L. Minnick, R. A. Flores, M. R. DeStefano, A. M. Scurto, *J. Phys. Chem. B* **2016**, *120*, 7906.
[7] R. P. Swatloski, S. K. Spear, J. D. Holbrey, R. D. Rogers, *J. Am. Chem. Soc.* **2002**, *124*, 4974.
[8] M. M. Jaworska, T. Kozlecki, A. Gorak, *J. Polym. Eng.* **2012**, *32*, 67.
[9] W. G. Glasser, R. H. Atalla, J. Blackwell, R. Malcolm Brown, W. Burchard, A. D. French, D. O. Klemm, Y. Nishiyama, *Cellulose* **2012**, *19*, 589.
[10] B. Medronho, A. Romano, M. G. Miguel, L. Stigsson, B. Lindman, *Cellulose* **2012**, *19*, 581.
[11] O. A. El Seoud, A. Koschella, L. C. Fidale, S. Dorn, T. Heinze, *Biomacromolecules* **2007**, *8*, 2629.
[12] D. M. Fox, W. H. Awad, J. W. Gilman, P. H. Maupin, H. C. De Long, P. C. Trulove, *Green Chem.* **2003**, *5*, 724.
[13] K. Fukumoto, M. Yoshizawa, H. Ohno, *J. Am. Chem. Soc.* **2005**, *127*, 2398.
[14] F. Hermanutz, F. Gaehr, E. Uerdingen, F. Meister, B. Kosan, *Macromol. Symp.* **2008**, *262*, 23.
[15] T. Heinze, K. Schwikal, S. Barthel, *Macromol. Biosci.* **2005**, *5*, 520.
[16] J. Wu, J. Zhang, H. Zhang, J. S. He, Q. Ren, M. Guo, *Biomacromolecules* **2004**, *5*, 266.
[17] H. Zhang, J. Wu, J. Zhang, J. S. He, *Macromolecules* **2005**, *38*, 8272.
[18] S. D. Zhu, Y. X. Wu, Q. M. Chen, Z. N. Yu, C. W. Wang, S. W. Jin, Y. G. Ding, G. Wu, *Green Chem.* **2006**, *8*, 325.
[19] C. Zhu, J. Chen, K. K. Koziol, J. W. Gilman, P. C. Trulove, S. S. Rahatekar, *eXPRESS Polym. Lett.* **2014**, *8*, 154.
[20] Y. Fukaya, A. Sugimoto, H. Ohno, *Biomacromolecules* **2006**, *7*, 3295.
[21] T. Mizumo, E. Marwanta, N. Matsumi, H. Ohno, *Chem. Lett.* **2004**, *33*, 1360.
[22] Y. Fukaya, K. Hayashi, M. Wada, H. Ohno, *Green Chem.* **2008**, *10*, 44.
[23] W. Normazlan, N. A. Sairi, Y. Alias, A. F. Udaiyappan, A. Jouyban, M. Khoubnasabjafari, *J. Chem. Eng. Data* **2014**, *59*, 2337.
[24] C. Zhu, R. M. Richardson, K. D. Potter, A. F. Koutsomitopoulou, J. S. van Duijneveldt, S. R. Vincent, N. D. Wanasekara, S. J. Eichhorn, S. S. Rahatekar, *ACS Sustainable Chem. Eng.* **2016**, *4*, 4545.
[25] M. Gericke, T. Liebert, T. Heinze, *Macromol. Biosci.* **2009**, *9*, 343.
[26] F. Huo, Z. P. Liu, W. C. Wang, *J. Phys. Chem. B* **2013**, *117*, 11780.
[27] J. M. Andanson, E. Bordes, J. Devemy, F. Leroux, A. A. H. Padua, M. F. C. Gomes, *Green Chem.* **2014**, *16*, 2528.
[28] Y. L. Zhao, X. M. Liu, J. J. Wang, S. J. Zhang, *J. Phys. Chem. B* **2013**, *117*, 9042.
[29] J. Zhang, H. Zhang, J. Wu, J. Zhang, J. He, J. Xiang, *Phys. Chem. Chem. Phys.* **2010**, *12*, 1941.
[30] L. Feng, Z.-l. Chen, *J. Mol. Liq.* **2008**, *142*, 1.
[31] K. Dong, S. Zhang, *Chem. - Eur. J.* **2012**, *18*, 2748.
[32] D. S. Zhao, H. Li, J. Zhang, L. L. Fu, M. S. Liu, J. T. Fu, P. B. Ren, *Carbohydr. Polym.* **2012**, *87*, 1490.
[33] R. C. Remsing, R. P. Swatloski, R. D. Rogers, G. Moyna, *Chem. Commun.* **2006**, 1271.
[34] J. Vitz, T. Erdmenger, C. Haensch, U. S. Schubert, *Green Chem.* **2009**, *11*, 417.
[35] A. Brandt, J. Grasvik, J. P. Hallett, T. Welton, *Green Chem.* **2013**, *15*, 550.
[36] H. Song, Y. Niu, Z. Wang, J. Zhang, *Biomacromolecules* **2011**, *12*, 1087.
[37] Z. Q. Luo, A. Q. Wang, C. Z. Wang, W. C. Qin, N. N. Zhao, H. Z. Song, J. G. Gao, *J. Mater. Chem. A* **2014**, *2*, 7327.
[38] L. K. J. Hauru, M. Hummel, A. W. T. King, I. Kilpeläinen, H. Sixta, *Biomacromolecules* **2012**, *13*, 2896.
[39] H. Sixta, A. Michud, L. Hauru, S. Asaadi, Y. B. Ma, A. W. T. King, I. Kilpelainen, M. Hummel, *Nord. Pulp Pap. Res. J.* **2015**, *30*, 43.
[40] A. Parviainen, A. W. T. King, I. Mutikainen, M. Hummel, C. Selg, L. K. J. Hauru, H. Sixta, I. Kilpelainen, *ChemSusChem* **2013**, *6*, 2161.
[41] H. Boerstoel, *Sen-I Gakkaishi* **2006**, *62*, P93.
[42] H. Boerstoel, H. Maatman, J. B. Westerink, B. M. Koenders, *Polymer* **2001**, *42*, 7371.
[43] H. Z. Song, J. Zhang, Y. H. Niu, Z. G. Wang, *J. Phys. Chem. B* **2010**, *114*, 6006.
[44] N. D. Wanasekara, A. Michud, C. C. Zhu, S. Rahatekar, H. Sixta, S. J. Eichhorn, *Polymer* **2016**, *99*, 222.
[45] S. J. Eichhorn, J. Sirichaisit, R. J. Young, *J. Mater. Sci.* **2001**, *36*, 3129.
[46] A. Michud, M. Tanttu, S. Asaadi, Y. Ma, E. Netti, P. Kääriainen, A. Persson, A. Berntsson, M. Hummel, H. Sixta, *Text. Res. J.* **2016**, *86*, 543.
[47] D. Ingildeev, F. Effenberger, K. Bredereck, F. Hermanutz, *J. Appl. Polym. Sci.* **2013**, *128*, 4141.
[48] M. M. Denn, *Annu. Rev. Fluid Mech.* **1980**, *12*, 365.
[49] X. W. Shi, Y. L. Hu, F. Y. Fu, J. P. Zhou, Y. X. Wang, L. Y. Chen, H. M. Zhang, J. Li, X. H. Wang, L. N. Zhang, *J. Mater. Chem. A* **2014**, *2*, 7669.
[50] X. Z. Dong, C. X. Lu, P. C. Zhou, S. C. Zhang, L. Y. Wang, D. H. Li, *RSC Adv.* **2015**, *5*, 42259.
[51] R. Ibbett, S. Gaddipati, S. Hill, G. Tucker, *Biotechnol. Biofuels* **2013**, *6*, 33; https://doi.org/10.1186/1754-6834-6-33.
[52] H. P. Fink, P. Weigel, H. J. Purz, J. Ganster, *Prog. Polym. Sci.* **2001**, *26*, 1473.
[53] S. S. Rahatekar, A. Rasheed, R. Jain, M. Zammarano, K. K. Koziol, A. H. Windle, J. W. Gilman, S. Kumar, *Polymer* **2009**, *50*, 4577.
[54] M. Ago, T. Endo, T. Hirotsu, *Cellulose* **2004**, *11*, 163.
[55] G. Cheng, P. Varanasi, R. Arora, V. Stavila, B. A. Simmons, M. S. Kent, S. Singh, *J. Phys. Chem. B* **2012**, *116*, 10049.
[56] S. Salmon, S. M. Hudson, *J. Macromol. Sci., Rev. Macromol. Chem. Phys.* **1997**, *C37*, 199.
[57] A. O'Sullivan, *Cellulose* **1997**, *4*, 173.
[58] L. Segal, J. J. Creely, A. E. Martin, C. M. Conrad, *Text. Res. J.* **1959**, *29*, 786.
[59] R. Y. Chen, K. A. Jakes, D. W. Foreman, *J. Appl. Polym. Sci.* **2004**, *93*, 2019.
[60] C. J. Garvey, I. H. Parker, G. P. Simon, *Macromol. Chem. Phys.* **2005**, *206*, 1568.
[61] A. D. French, *Cellulose* **2014**, *21*, 885.
[62] S. Park, J. Baker, M. Himmel, P. Parilla, D. Johnson, *Biotechnol. Biofuels* **2010**, *3*, 10.
[63] M. G. Northolt, H. Boerstoel, H. Maatman, R. Huisman, J. Veurink, H. Elzerman, *Polymer* **2001**, *42*, 8249.
[64] S. J. Eichhorn, R. J. Young, R. J. Davies, C. Riekel, *Polymer* **2003**, *44*, 5901.